

Analysis of Stress Intensity Factors for Mode I and Mixed Mode with Digital Image Correlation

ME EN 6960

Nik Benko, John Callaway, Nick Dorsett, Martin Raming

March 26, 2018

Abstract

1 Introduction

2 Methods

2.1 Experimental Techniques

2.1.1 Digital Image Correlation

DIC is a commonly used optical technique in experimental mechanics to accurately measure full-field displacements, and rotations by capturing a sequence of images of the surface in question. Using two cameras these measurements can be taken in 3D. If only 2D measurements are needed, as in this experiment, only one camera is needed for imaging the surface.

An initial digital image is taken before any loading to be used as the reference image. Here it is assumed that there are zero displacements, or rotations. This reference image is then compared to a digital

image taken once loading has occurred, also known as the deformed image. In many cases numerous digital images are captured during loading for comparison to create a sequence of displacements and rotations. For correlation to take place an area of interest within the images is selected and then divided into square sections known as subsets. Each subset is made up of the same number of pixels. The subsets are matched in the reference and deformed images through a correlation function within the DIC algorithm. By corresponding each pixel to an actual unit of length deformations and rotations can then be tracked using a DIC algorithm.

For the DIC algorithm to be effective each subset must contain enough unique features. These features are related to contrast or pixel values. A high-contrast grainy surface is desired to create such usable features. In practice this is known as the speckle pattern. A good speckle pattern consists of a uniformly dispersed speckles of random shapes and varying sizes. The size of the speckles needed will depend on the size of the specimen and focusing distances. For example a small specimen with the camera close will require very small speckles while a larger specimen with the camera backed off larger speckles are needed.

2.1.2 Experimental Determination of Displacement Fields

Mode I displacement fields can be obtained by loading a specimen that has an edge crack in a three point configuration. This configuration and specimen geometry is given in Figure 7. Alignment of the roller directly above the crack tip creates pure bending around the crack, which induces only mode I crack opening, and therefore mode I displacement fields.

Mixed mode displacement fields can be obtained by inducing eccentricity in the previously described three point loading configuration. This can be done by moving one of the lower support rollers, creating a combination of bending (Mode I) and shear (Mode II) around the crack. This configuration is given in Figure 8.

2.1.3 Calculation of Stress Intensity Factors

Theoretical mode I stress intensity factors (K_I) can be calculated using the closed form equation:

$$K_I = Y\sigma\sqrt{\pi a} \quad (1)$$

where σ is the farfield stress, a is the crack length and Y is a geometric factor specific to the loading configuration and specimen geometry. Using the solution developed in *The Stress Analysis of Cracks Handbook*, the stress intensity factor for the single edge notched bend specimen being examined is:

$$K_I = \frac{P}{B\sqrt{W}} \left(\frac{\frac{3S}{W}\sqrt{\frac{a}{w}}}{2(1 + \frac{2a}{w})(1 - \frac{a}{w})^{1.5}} \right) \left[1.99 - \frac{a}{w} \left(1 - \frac{a}{w} \right) \left[2.15 - 3.93 \left(\frac{a}{w} \right) + 2.7 \left(\frac{a}{w} \right)^2 \right] \right] \quad (2)$$

where P is the applied load, W is the specimen width, B is the specimen thickness and a is the crack length.

Experimental mode I stress intensity factors can be found using the experimental displacement fields. From the Westergaard solution, the displacements around the crack can be described by the following equations:

$$u_x = \frac{K_I}{8\mu\pi} \sqrt{2\pi r} \left[(2\kappa - 1) \cos\left(\frac{\theta}{2}\right) - \cos\left(\frac{3\theta}{2}\right) \right] \quad (3)$$

$$u_y = \frac{K_I}{8\mu\pi} \sqrt{2\pi r} \left[(2\kappa + 1) \sin\left(\frac{\theta}{2}\right) - \sin\left(\frac{3\theta}{2}\right) \right] \quad (4)$$

where (r,θ) are the polar coordinate of the point, μ is the shear modulus and κ is $\frac{3-\nu}{1+\nu}$ (ν is Poisson's ratio) for the plane stress state of the experiment.

Mixed mode stress intensity factors can also be found using the experimental mixed mode displacement fields. The displacement field for a combined Mode I and Mode II loading situation is the sum of the displacements for each individual loading condition, as given by the following equations:

$$u_x = \frac{K_I}{8\mu\pi} \sqrt{2\pi r} \left[(2\kappa - 1) \cos\left(\frac{\theta}{2}\right) - \cos\left(\frac{3\theta}{2}\right) \right] + \frac{K_{II}}{8\mu\pi} \sqrt{2\pi r} \left[(2\kappa + 3) \sin\left(\frac{\theta}{2}\right) + \sin\left(\frac{3\theta}{2}\right) \right] \quad (5)$$

$$u_y = \frac{K_I}{8\mu\pi} \sqrt{2\pi r} \left[(2\kappa + 1) \sin\left(\frac{\theta}{2}\right) - \sin\left(\frac{3\theta}{2}\right) \right] - \frac{K_{II}}{8\mu\pi} \sqrt{2\pi r} \left[(2\kappa - 3) \cos\left(\frac{\theta}{2}\right) + \cos\left(\frac{3\theta}{2}\right) \right] \quad (6)$$

Thus, individual K_I and K_{II} values can be solved by solving the system of equations with the known displacement values at any given point.

2.2 Procedure

The experiment was conducted with a thin rectangular PMAA (acrylic) specimen . To simulate a crack the specimen was cut with a bandsaw directly in the center to a length of ???. This method was chosen to allow for a blunt crack tip so that premature failure of the specimen does not occur while testing. One side of the plate was painted completely white and then speckled using a black aerosol paint. The black paint was applied in a way that allowed for random speckling with in a size range that would allow for proper DIC measurements.

To extract mode I data the specimen was placed in a three-point bend fixture with in an electronic screw-driven Instron machine as figure ? shows. A light load of about 7N was used to hold the specimen in place. The DIC setup consisted of one camera with ??mm lens mounted to a tripod. Two green lights with flexible attachments were positioned and aligned to provide adequate lighting. With the DIC system in place the aperture to the camera was opened fully and the camera lens was then focused referencing the area around the crack tip. Next the aperture and light control were adjusted so that focus was maintained with no over exposure.

We then took several images to obtain an initial reference and to get an estimate of unwanted noise. From here we incremented the load on the specimen while subsequently taking an image at each increment. Care was taken to record the load as close to the point in time that the image was captured since the specimen would relax with in the fixture resulting in a steady decreasing load. Once the threshold of 300N was reached we unloaded the specimen. For mixed mode load we adjusted the three-point fixture to create asymmetric loading. This was achieved by simply moving one support towards the center. This lead to a gap of four inches from one support to the center on one side and two inches on the other. Just as before

the camera was focused and adjusted following incremental loading with correlated images. Table ?? shows the sequence for each load and the correlated image number for both mode I and mode II.

2.3 Error and Uncertainties

3 Results

In total, eight images were recorded and analyzed for each loading scenario. DIC was used to calculate u_x and u_y for each of the eight load increments. Rectangular sub-regions surrounding the crack were selected for analysis. Signal to Noise Ratio tended to decrease with increased load so analysis was focused on the 1010 N load increment. Equation 3 and Equation 4 were inverted to solve for K_I and experimental displacement fields were used to create contour plots of K_I , shown in Figure 1 and Figure 2. Inverting these equations created singularities as the denominator trended towards 0 at $\theta = \pm\pi$, so values exceeding 10 were eliminated to increase contrast.

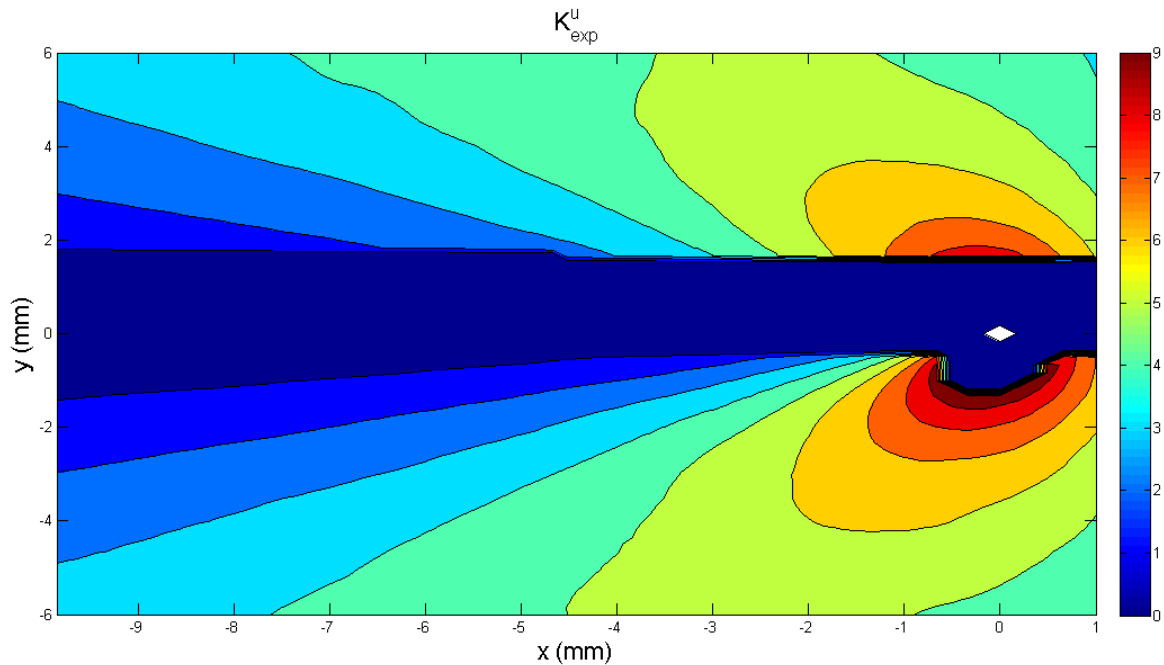


Figure 1: Contour plot of experimental values K_I^U . Values above 10 have been set to 0 for clarity

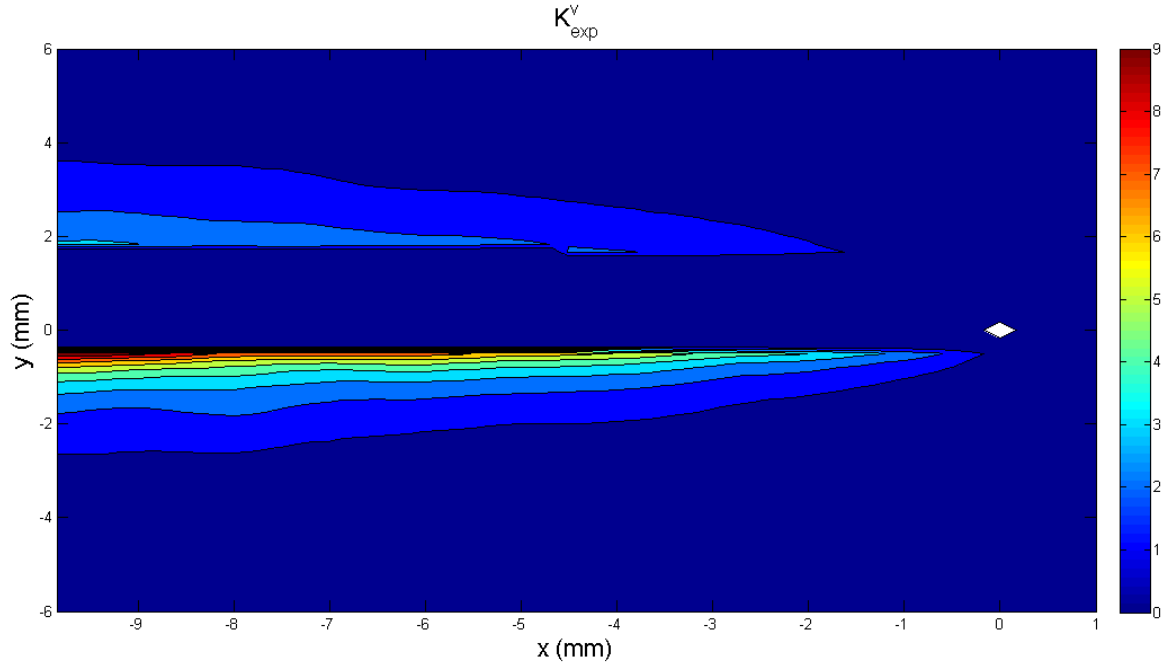


Figure 2: Contour plot of experimental values K_1^V . Values above 10 have been set to 0 for clarity

Experimental K_I values were observed to be highly dependent on location. K_I became less accurate as distance from the crack increased for values calculated from u_x data. The opposite relation was observed for u_y data. To analyze how well theoretical K_I fit the experimental data, two points along the x-axis on the $K_I^{u_x}$ plot were chosen for further analysis. K_I was then calculated for each of the eight load increments. Results are shown in Figure 3. K_I at both locations closely matched predicted values with $R^2 > 0.98$ in both cases.

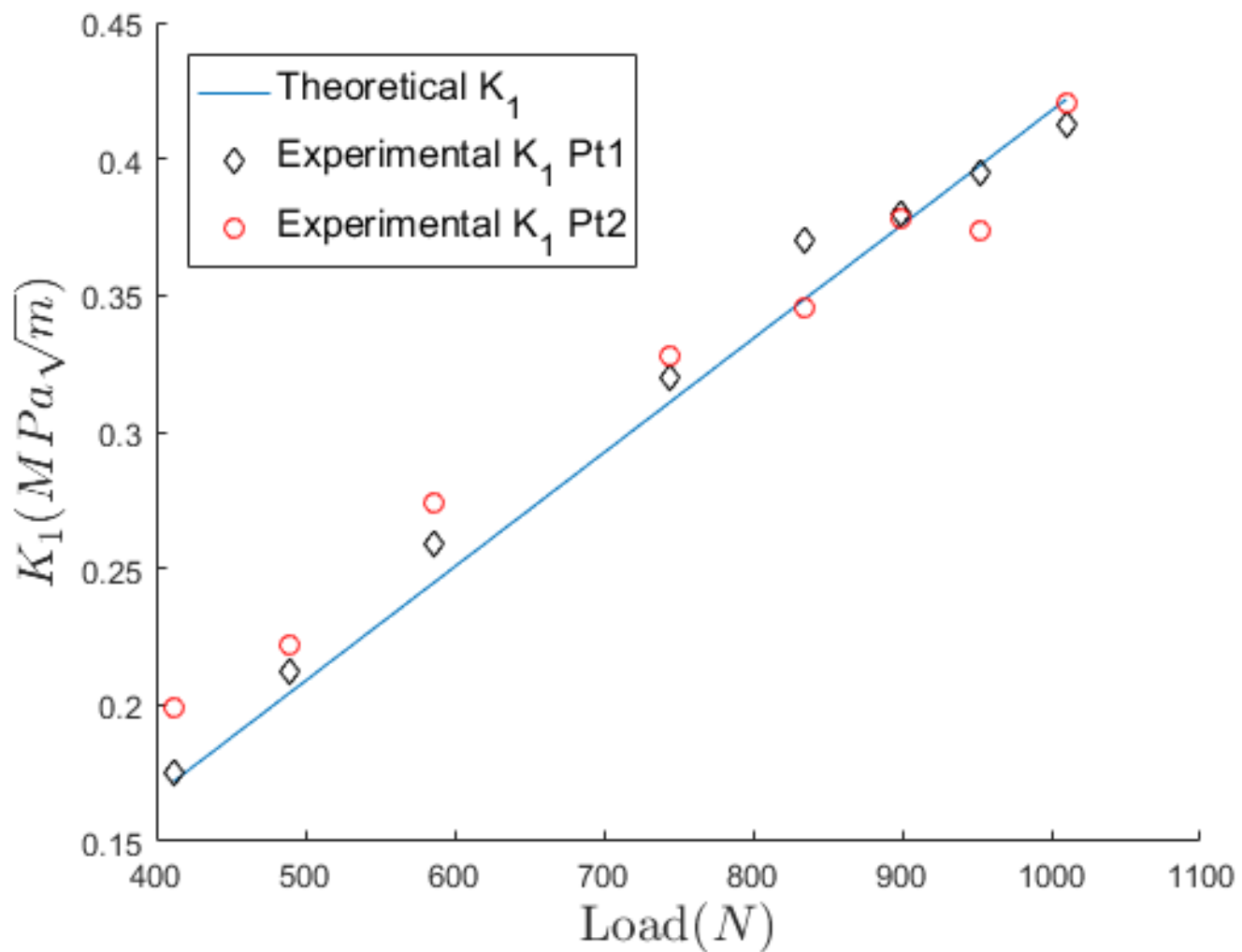


Figure 3: Theoretical and experimental mode I stress intensity factor at two points along the x-axis.

Contour plots of raw u_x and u_y displacement data were drawn and shown in Figure ?? and Figure 5.

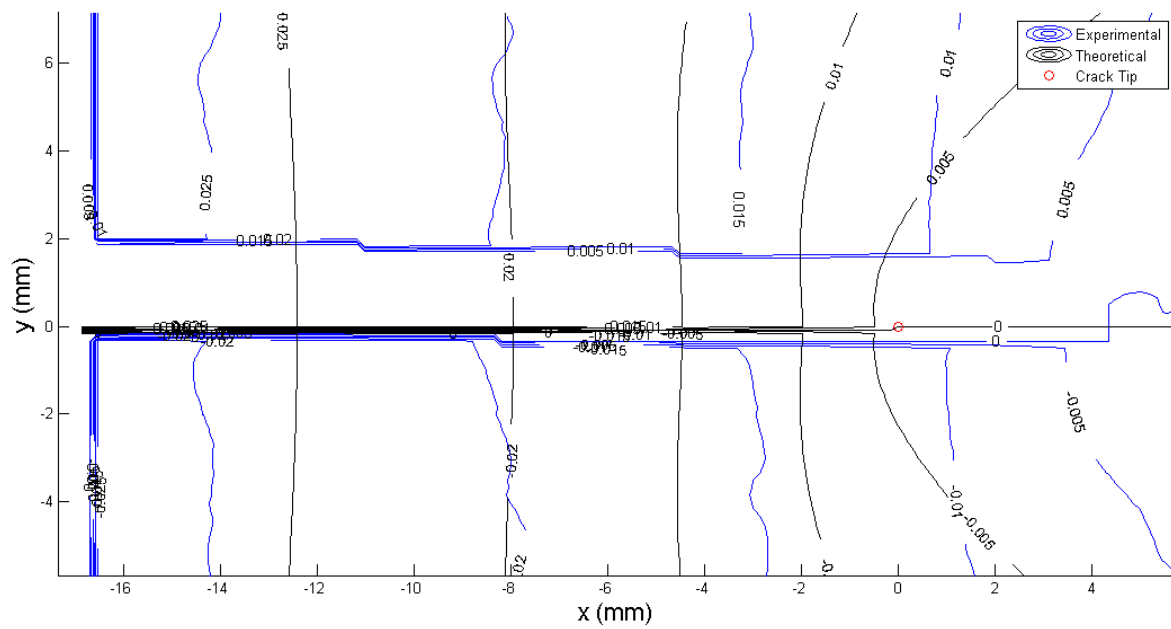


Figure 4: Comparison between theoretical and experimental U displacements

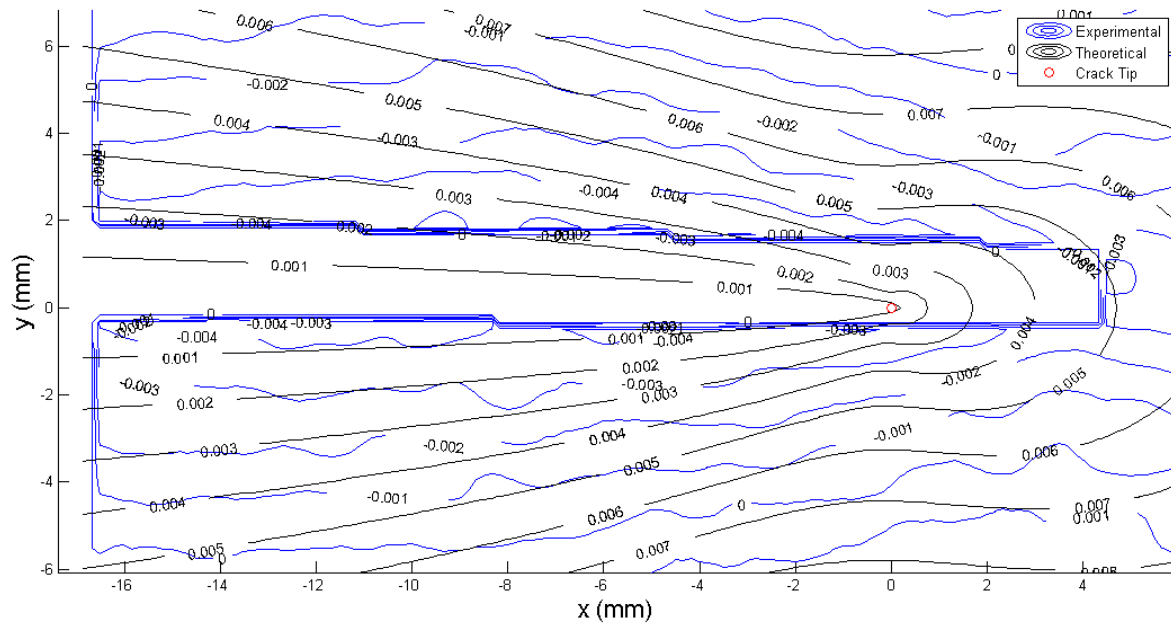


Figure 5: Comparison between theoretical and experimental V displacements

4 Discussion

The general shape of both u_x and u_y fields in Mode I tests matched well with predictions. Field magnitudes also agreed closely, but spacing between contour lines did not always match perfectly. The roughness in experimental contours is likely due to errors inherent in DIC methods such as finite pixel/speckle size and subset selection. There are several possible explanations for disagreements in contour spacing. First, theoretical calculations depend on bulk modulus, μ , which was not measured, but derived from Young's Modulus and Poisson's ratio, taken from on-line sources. Additionally, theoretical calculations assume an infinitely thin crack with a sharp tip. The test specimen crack was cut with a band saw and therefore has a finite width and a blunted tip.

5 Conclusion

6 Figures

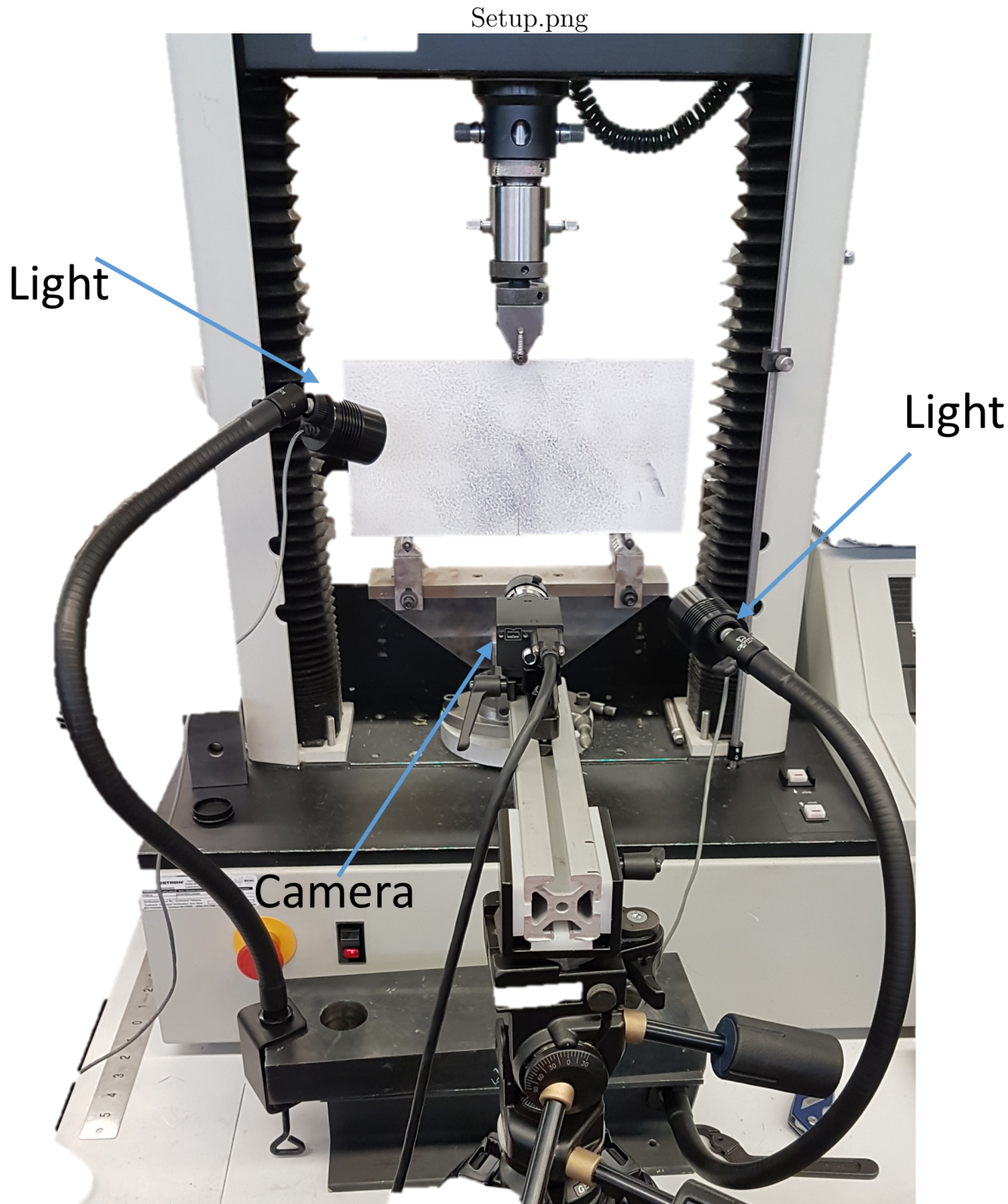


Figure 6: The specimen is mounted to the fixture with the DIC system in place, here the camera is fixed to a tripod and two adjustable lights are seen on either side.

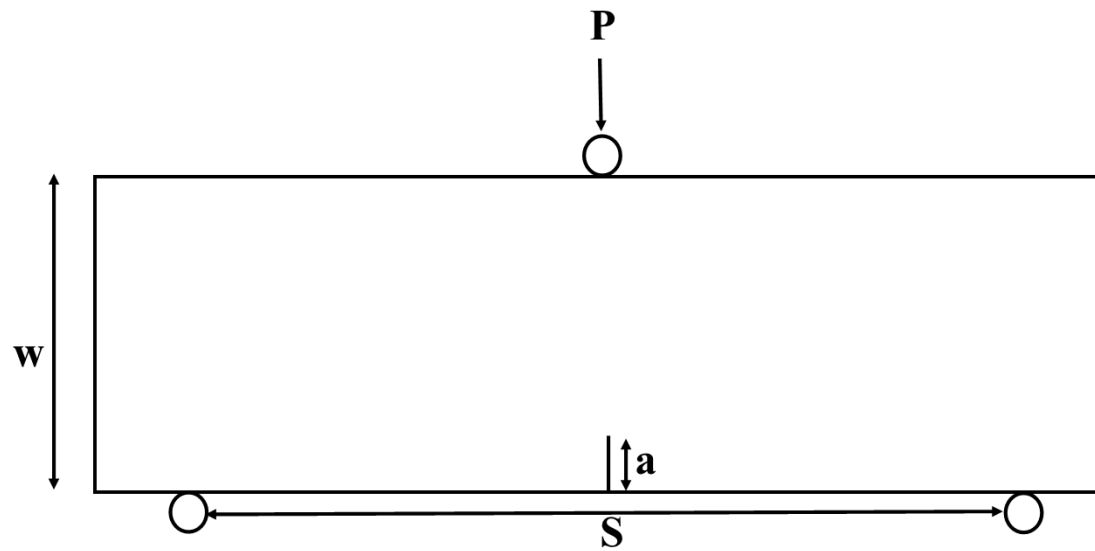


Figure 7: Three point loading configuration of specimen, where $S = 0.2032$ m, $w = 0.1524$ m, $a = 0.0254$ m and a specimen thickness (B) of 0.00875 m. Applied load, P , is applied to the top roller

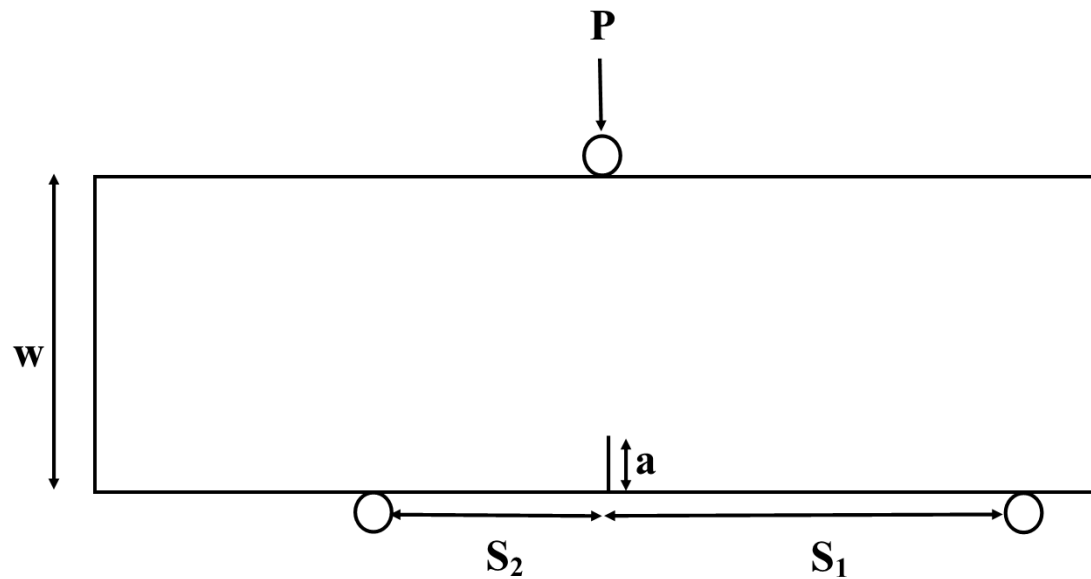


Figure 8: Three point loading configuration of specimen, where $S_1 = 0.1016$ m, $S_2 = 0.0508$ m, $w = 0.1524$ m, $a = 0.0254$ m, and a specimen thickness (B) of 0.00875 m. Applied load, P, is applied to the top roller

7 Tables

8 Appendix

8.1 Code

References